Biochimica et Biophysica Acta 1778 (2008) 2573–2579

Contents lists available at ScienceDirect

Biochimica et Biophysica Acta

journal homepage: www.elsevier.com/locate/bbamem

Membrane tension regulates water transport in yeast

Graça Soveral [a,b,*], Ana Madeira [a], Maria C. Loureiro-Dias [c], Teresa F. Moura [a]

[a] REQUIMTE, Dep. Química, FCT-UNL, 2829-516 Caparica, Portugal
[b] Faculdade de Farmácia, Universidade de Lisboa, 1649-003 Lisboa, Portugal
[c] Instituto Superior de Agronomia, Universidade Técnica de Lisboa, 1349-017 Lisboa, Portugal

ARTICLE INFO

Article history:
Received 17 March 2008
Received in revised form 17 July 2008
Accepted 17 July 2008
Available online 29 July 2008

Keywords:
Yeast
Saccharomyces cerevisiae
Water transport regulation
Aquaporin
Membrane tension

ABSTRACT

Evidence that membrane surface tension regulates water fluxes in intact cells of a *Saccharomyces cerevisiae* strain overexpressing aquaporin *AQY1* was obtained by assessing the osmotic water transport parameters in cells equilibrated in different osmolarities. The osmotic water permeability coefficients (P_f) obtained for yeast cells overexpressing *AQY1* incubated in low osmolarity buffers were similar to those obtained for a double mutant *aqy1aqy2* and approximately three times lower (with higher activation energy, E_a) than values obtained for cells incubated in higher osmolarities (with lower E_a). Moreover, the initial inner volumes attained a maximum value for cells equilibrated in lower osmolarities (below 0.75 M) suggesting a pre-swollen state with the membrane under tension, independent of aquaporin expression. In this situation, the impairment of water channel activity suggested by lower P_f and higher E_a could probably be the first available volume regulatory tool that, in cooperation with other osmosensitive solute transporters, aims to maintain cell volume. The results presented point to the regulation of yeast water channels by membrane tension, as previously described in other cell systems.

1. Introduction

Evidence for the existence of water channels in cell membranes was first obtained for red blood cells (RBCs) [1–4] and renal epithelia [5] and was based mainly on measures of high osmotic water permeability (inhibited by mercurial reagents) and of low activation energy (E_a) for water transport. In 1992 Agre et al. identified the first aquaporin known as aquaporin 1 (AQP1) [6] and since then the structure and function of aquaporins in animals, plants and microbes have been extensively studied. Aquaporins belong to a highly conserved group of membrane proteins called the major intrinsic proteins (MIPs) that are widely spread in nature, with important functions in water homeostasis and osmoregulation of individual cells and whole organisms. The gating of water channels by high concentration of osmotic solutes [7] and by mechanical stimuli [8] has been recently reported in plants. Factors like phosphorylation, pH, pressure, solute gradients and temperature among others were reported to affect the gating behaviour of plant water channels [9].

In microorganisms, aquaporins were also recognized but their physiological role is yet being explored [10]. The functionality of aquaporins Aqy1p and Aqy2p in *Saccharomyces cerevisiae* has been in debate in the literature. Aquaporin deletion strains revealed to be more resistant to rapid changes in osmolarities [11,12]. However, inactivation of the aquaporin genes [11,13] has no evident effect on growth under a variety of conditions. A functional role of the Aqy1p in the formation of spores has been demonstrated [14]. In addition, a substantial increase in survival upon rapid freezing [15] and a relevant aquaporin activity restricted to low temperature [16] have been found in strains with altered expression of aquaporin genes. All these findings regarding the physiological roles and regulation of yeast aquaporins are puzzling and require further elucidation.

It is now recognized that under extreme conditions many cells exhibit active control of their volume responding to hypo or hypertonic challenges by unloading or loading ions or other solutes to recover their original volume by osmosis [17,18]. However, the enhanced water permeability conferred by aquaporin, actually would work against the control of cell volume, amplifying the perturbations produced by changes in osmotic gradients and making homeostasis more difficult and volume changes more drastic within a short time span, even if the uptake and synthesis of osmolytes pathway were triggered [19]. This aspect of aquaporin physiology seems to be controversial unless a compensation mechanism of channel regulation would be present. In fact, inhibition of water channels by an increase in membrane surface tension has been demonstrated in mammalian kidney brush border vesicles, prepared from proximal tubule cells [20]. Based on this finding, a simple mechanism for volume regulation in this bipolar epithelial tissue, where massive solute and fluid transport occur, has been proposed [21], conferring to water channels a volume regulatory role alternative to solute transport mechanisms.

The goal of the present study was to access the role of water channel as an equivalent volume regulator in yeast cells. Experimental conditions were designed in order to create increasing levels of

* Corresponding author. Tel.: +351 212948385; fax: +351 212948550.
E-mail address: soveral@dq.fct.unl.pt (G. Soveral).

0005-2736/$ – see front matter © 2008 Elsevier B.V. All rights reserved.
doi:10.1016/j.bbamem.2008.07.018

membrane tension and evaluate their effect on water channel activity. We chose a yeast strain overexpressing *AQY1*, whose phenotype associated with aquaporin overexpression was previously characterized for a broad temperature range, and a double mutant *aqy1aqy2*. The wild strain is not suitable to study the properties of water channels, since it displays a poor activity of mediated water transport [16].

A non-invasive fluorescence self-quenching method was used to follow intact cell volume changes subsequent to osmotic shocks [22]. The experimental protocols tested involved the equilibration of cells in different media osmolarities in order to create different internal hydrostatic pressures that would induce different levels of membrane surface tension. Using an analysis that incorporates both osmotic and hydrostratic pressures, the osmotic permeability coefficient (P_f) and the activation energy for water transport (E_a) of both strains were calculated and compared under different experimental conditions. A decrease in P_f and increase in E_a correlated with the establishment of experimental membrane tension was found only for the *AQY1* overexpressing strain. We suggest that aquaporin inhibition by membrane tension may play a role in yeast volume regulation.

2. Materials and methods

2.1. Yeast strains

The strains used in this work were 10560-6B/pYX012 *KanMX AQY1-1 MATα leu2::hisG trp1::hisG his3::hisG ura3-52* (= strain ANT27, further indicated as strain AQY1) and 10560-6B *aqy1::KanMX4 aqy2::HIS3* (= strain YSH 1172, further indicated as double mutant *aqy1aqy2*) [23], kindly provided by Prof. Patrick Van Dijck, Institute of Botany and Microbiology, Katholieke Universiteit Leuven and Flanders Interuniversity Institute for Biotechnology (VIB), Kasteelpark Arenberg, Belgium.

2.2. Cell culture and fluorophore loading

Cells were grown in YPD medium (1% (w/v) peptone, 0.5% (w/v) yeast extract, 2% (w/v) glucose), with orbital shaking, at 28 °C. Cells were harvested in the exponential phase ($OD_{640} \approx 1$) by centrifugation (10 000 rpm) for 3 min at 4 °C, washed once and resuspended in sorbitol solutions with osmolarities osm_{out} = 0.1, 0.2, 0.3, 0.4, 0.5, 0.75, 1, 1.4 M and kept on ice. Prior to the osmotic challenges the cells were pre-loaded for 10 min at 30 °C with the nonfluorescent precursor 5-and-6-carboxyfluorescein diacetate (CFDA, 1 mM in isoosmotic solution) that is cleaved intracellularly by nonspecific esterases and generates the impermeable fluorescent form known to remain in the cytoplasm. To avoid pH interference in fluorescence, cell suspensions and osmotic solutions were prepared in K^+-citrate buffer (50 mM, pH 5).

2.3. Cell volume determination

Equilibrium volumes of CFDA loaded cells were obtained under an epifluorescent microscope (Olympus BX51) equipped with a digital camera. Cells were assumed to have a spherical shape with a diameter calculated as the average of the maximum and minimum dimensions of each cell. Cells were exposed to osmotic shocks of increasing tonicity on a microscope slide, an average of 6 pictures with 4–6 cells each were taken before (V_o) and within 10 to 40 s after the osmotic challenge (V_∞). The tonicity of the osmotic shock is defined as the ratio of the final to initial osmolarity of the outside medium, $\Lambda = (osm_{out})_\infty / (osm_{out})_o$.

Using a *Boyle–van't Hoff plot*, the non-osmotic volume (β) was determined by plotting the initial cell volume (V_o) as a function of the reciprocal initial osmolarity (osm_{out}). β was taken as the intercept with the volume axis of the regression line to the experimental points.

2.4. Stopped-flow fluorescence experiments

Stopped-flow technique was used to monitor cell volume changes of cells loaded with a concentration-dependent self-quenching fluorophore [22]. Experiments were performed on a HI-TECH Scientific PQ/SF-53 stopped-flow apparatus, which has a 2 ms dead time, temperature controlled, interfaced with an IBM PC/AT compatible 80386 microcomputer. Experiments were performed at temperatures ranging from 7 to 38 °C. Three runs were usually stored and analyzed in each experimental condition. In each run 0.1 ml of cell suspension (1:10 dilution in resuspension buffer) was mixed with an equal amount of hypo or hyperosmotic sorbitol solutions to reach different out or inwardly directed solute gradients. Fluorescence was excited using a 470 nm interference filter and detected using a 530 nm cut-off filter and the changes in fluorescence due to carboxyfluorescein (CF) fluorescence quenching were recorded.

The calibration of the fluorescence stopped-flow traces (F) into cell volume (V) was done using the experimentally obtained linear relation between V and F.

2.5. Evaluation of osmotic permeability coefficients

The evaluation of P_f followed a strategy developed for plasma membrane vesicles [20] adapted here for intact cells, where the non-osmotic volume β is taken into account. Briefly, the osmotic water flow J_v out of a cell whose osmotic volume is V_{osm} (calculated as $V_{osm} = V - \beta$) and surface area is A is proportional to the sum of the hydrostatic ($\Delta P = P_{in} - P_{out}$) and osmotic ($\Delta\Pi = RT\,(osm_{in} - osm_{out})$) pressure differences, where RT is the gas constant times the absolute temperature. Letting P_f denote the osmotic permeability coefficient and V_w the partial molar volume of water, the calculated volume flow is:

$$J_v = -\frac{dV_{osm}}{Adt} = P_f V_w \left(\frac{\Delta P - \Delta\Pi}{RT}\right). \quad (1)$$

Knowing that β is a constant, then $dV_{osm}/dt = d(V-\beta)/dt = dV/dt$. Convenient dimensionless variables can be obtained by utilizing the initial volume V_o and $(osm_{out})_o$ as normalizing factors, and defining:

$$\left.\begin{array}{l} v = V/V_o \\ p = \Delta P/(RT(osm_{out})_o) \\ \Lambda = (osm_{out})_\infty/(osm_{out})_o \end{array}\right\} \quad (2)$$

Taking these relations into account and rearranging Eq. (1),

$$\frac{dv}{dt} = \frac{A}{V_o} P_f V_w (osm_{out})_o \left[\left(\frac{osm_{in}}{(osm_{out})_o} - p\right) - \Lambda\right]. \quad (3)$$

Considering the osmotic equilibrium at departure and taking into account that during the osmotic perturbation all solutes are considered impermeant (and only reside in the osmotic volume), the term in parenthesis can be reduced to a "*function*" of v,

$$\left.\begin{array}{l} \left(\frac{osm_{in}}{(osm_{out})_o} - p\right) = \left(\frac{p_o + 1}{v_{osm}} - p\right) = function \\ v_{osm} = \frac{v - \beta/v_o}{1 - \beta/v_o} \end{array}\right\} \quad (4)$$

where v_{osm} is the relative osmotic volume, p_o is the initial value of p for each cell population and these variables are all dependent on $(osm_{out})_o$ and on v. Replacing this expression on Eq. (3), the final equation obtained is

$$\frac{dv}{dt} = \frac{A}{V_o} P_f V_w (osm_{out})_o (function - \Lambda). \quad (5)$$

For a given osmotic shock experiment where cells equilibrated in a medium of osmolarity $(osm_{out})_o$ are suddenly exposed to a new

medium with osmolarity $(osm_{out})_\infty$, the osmotic permeability coefficient P_f (and the hydraulic permeability, $L_p = P_f\ V_w/RT$) can be estimated by numerically integrating Eq. (5) and curve fitting the results to calibrated stopped-flow traces, using the "*function*" dependence on $1/v$ obtained by plotting Λ vs. $1/v$ taken from microscopy volume measurements.

Numerical integrations as well as curve fitting were accomplished with the Berkeley Madonna software (http://www.berkeleymadonna.com/). The activation energy (E_a) of water transport was evaluated from the slope of the Arrhenius plot ($\ln P_f$ as a function of $1/T$).

3. Results

3.1. Membrane tension arises in low osmolarity media

Fig. 1A shows the inner volumes of cell preparations of *S. cerevisiae* (strains AQY1 and double mutant) equilibrated in different initial osmolarities (V_o) and subjected to large hypertonic shocks that induce considerable volume changes (V_∞). It is apparent that, in both strains, the initial inner volume V_o of these cells reached their maximum value ($22.24 \pm 1.00\ \mu m^3$) for cells equilibrated in low osmolarity buffers

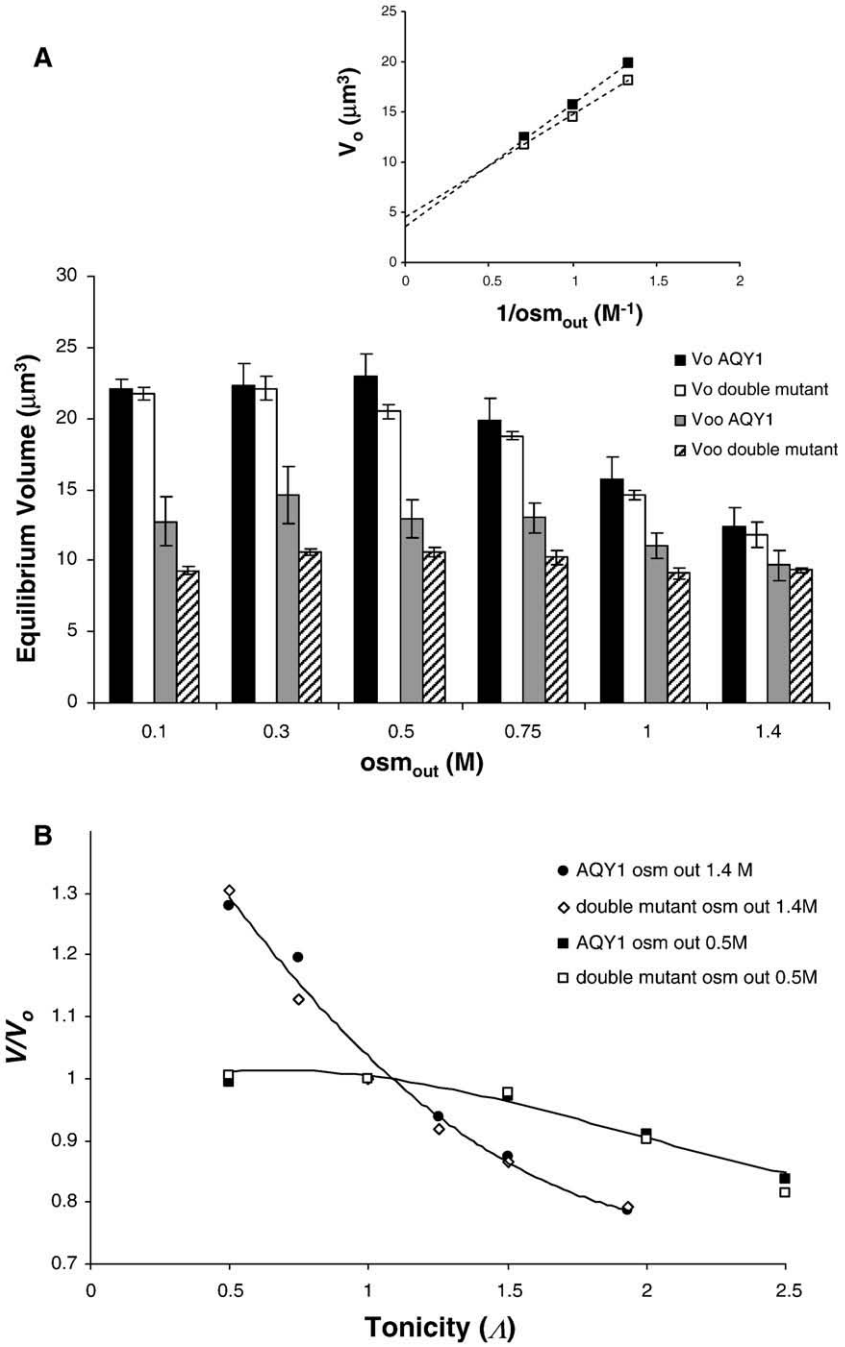

Fig. 1. Equilibrium cell volumes of *S. cerevisiae* (overexpressing *AQY1* and double mutant *aqy1aqy2* strains). (A) Inner volumes of cell preparations equilibrated in different initial osmolarities (V_o) and subjected to large hypertonic shocks that induce considerable volume changes (V_∞). Data shown are mean ± SD of triplicates of three independent experiments. Inset: Boyle–van't Hoff plot to determine the non-osmotic volume ($\beta = 3.62\ \mu m^3$ and $4.31\ \mu m^3$ for the AQY1 and double mutant respectively). (B) Typical pattern of the relative volume change (V/V_o) for cells equilibrated in 1.4 M (● AQY1 and ◇ double mutant) and in 0.5 M (■ AQY1 and □ double mutant) subjected to hypo- and hypertonic shocks.

(below 0.5 M). These results suggest the building up of membrane tension independent of aquaporin expression. The final volume V_∞, obtained when these cells were subjected to high tonicity within acceptable limits, tended to a minimum value ($9.52 \pm 0.95\ \mu m^3$). The determination of the non-osmotic volume (β) of these cells was achieved using a Boyle–van't Hoff plot (Fig. 1A inset). The V_o values from the cells equilibrated in the higher osmolarity medium (above 0.5 M) were plotted vs. the corresponding reciprocal of osm_{out} and equivalent values of β ($3.62\ \mu m^3$ for the AQY1strain and $4.31\ \mu m^3$ for the double mutant) were taken from the intercepts of the linear fits to the data points. These values are lower than the V_∞ measured for all the cell preparations, as it would be expected for the osmotic shocks applied.

When comparing the relative change in cell volume (V/V_o) obtained for cells equilibrated in different initial osmolarities and subjected to the same tonicity shock (hypo and hyperosmotic) a diverse behaviour was obtained. Cells equilibrated in the low osmolarity media (<0.75 M) did not respond to hypotonic shocks, and had a much smaller response to hypertonic shocks compared with cells equilibrated in the higher osmolarity solutions. A typical pattern of the relative volume change (V/V_o) observed under fluorescence microscopy is shown in Fig. 1B for both AQY1 and double mutant strains under two experimental conditions (0.5 and 1.4 M). For the hypotonic shocks, the volume change was negligible for cells equilibrated in 0.5 M while cells equilibrated in 1.4 M showed measurable volume changes, reaching a 30% increase in cell volume for a Λ=0.5. This same behaviour was observed for hypertonic shocks

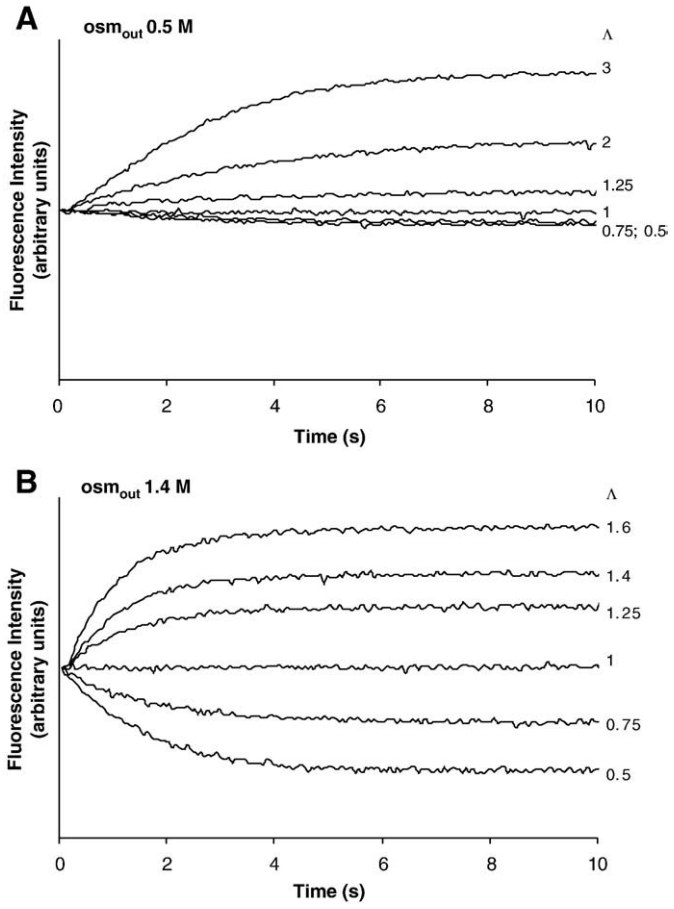

Fig. 2. Time course of volume change, followed by fluorescence stopped-flow, for *AQY1* overexpressing cells. (A) Equilibrated in 0.5 M and (B) equilibrated in 1.4 M. The curves are identified by the tonicity of the osmotic shock (Λ). The same arbitrary units are used in (A and B).

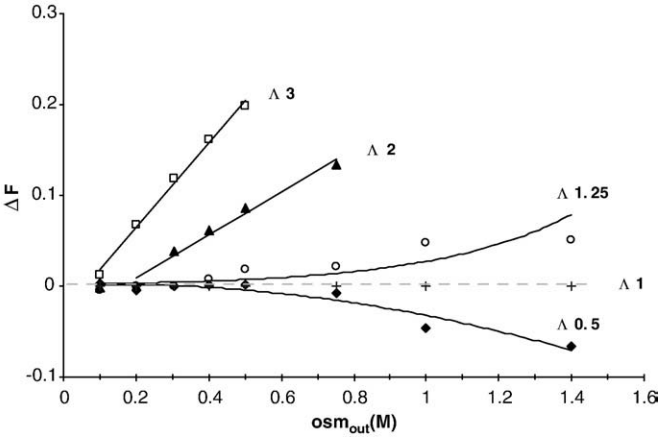

Fig. 3. Total change in stopped-flow fluorescence (ΔF) for typical osmotic challenges (curves Λ 0.5 (♦), Λ1.0 (+), Λ 1.25 (○), Λ 2 (▲) and Λ 3 (□)) as a function of the initial external media osmolarity osm_{out} obtained for *AQY1* overexpressing strain. Identical data was obtained for the double mutant *aqy1aqy2*.

where, for the same tonicity, the relative volume change was always more prominent for the 1.4 M populations. For instance, Λ=2 shock induced a decrease in cell volume up to 22% of the initial value for the 1.4 M populations, while for the 0.5 M the decrease was only up to 10%.

The time course of volume change for cells equilibrated in the different external solutions and exposed to different tonicity shocks was followed by stopped-flow fluorescence. Fig. 2A and B show the fluorescence traces obtained for AQY1 cells equilibrated in 0.5 and 1.4 M. The curves are identified by the tonicity of the osmotic shock (Λ). It can be observed from the signal amplitude that cells equilibrated in the lower osmolarity medium show impaired volume changes for the hypotonic and for the lower hypertonic shocks, compared with volume changes observed for the 1.4 M equilibrated cells. Equivalent traces but with a slower time course were obtained for the double mutant (data not shown). These observations agree with the volume change measured by fluorescence microscopy described above.

Fig. 3 shows the curves corresponding to the total change in fluorescence ($\Delta F = F_\infty - F_o$) for typical osmotic challenges (Λ=0.5, 1, 1.25, 2 and 3), as a function of the initial external media osmolarity, osm_{out}. It can be observed from the change in ΔF, that only cells pre-equilibrated in higher osmolarities (osm_{out}>0.75 M) swell for the hypotonic shock (curve Λ=0.5) and shrink for the lowest hypertonic shock (curve Λ=1.25). Cells equilibrated in lower osmolarities (osm_{out}<0.5 M) required higher hypertonic shocks to change their volume. In fact, changes in fluorescence (ΔF) were only detected if cells were subjected to osmotic shocks of higher magnitudes, e.g., Λ=2 for cells in 0.3 M and Λ=3 for cells in 0.2 M. Cells equilibrated in 0.1 M could only respond to osmotic challenges above Λ=3 (data not shown).

This set of results indicates that cells equilibrated in low osmolarity media develop a membrane surface tension that keeps the cells in a swollen state. This is a mechanical property of yeast cell structure that is independent of aquaporin expression. Under these conditions, cells are unable to change their volume upon hypotonic shocks.

3.2. Calibration of stopped-flow traces and Pf evaluation

The fluorescence intensity signals were calibrated using the linear relation shown in Fig. 4 between the relative change in cell volume V/V_o, and the output signal F, *i.e.* $V/V_o = a\ F + b$, where V is the cell volume attained after an osmotic perturbation from its original volume V_o, and a and b are constants. In Fig. 4 the fluorescence data F_∞ (from stopped-flow traces) is plotted against the corresponding measured volumes V_∞/V_o (from microscopy data) for cells equilibrated in the

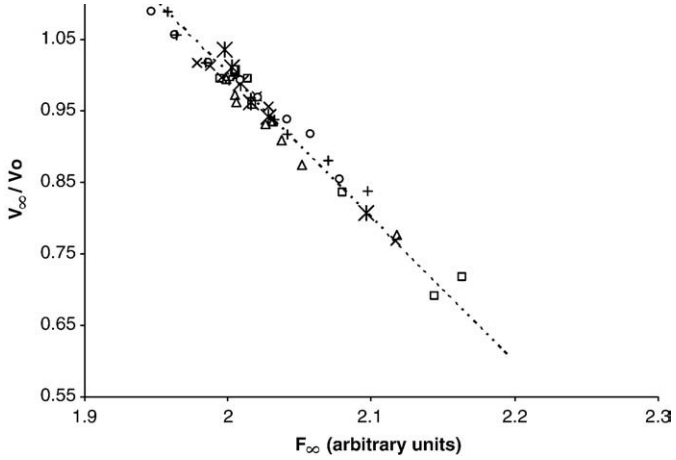

Fig. 4. Relation between the relative change in cell volume V_∞/V_o (from microscopy data) and the output fluorescence signal F_∞ (from stopped-flow traces) for cells equilibrated in the different osm_{out} (0.1 to 1.4 M) and subjected to different tonicity shocks. All the data points fall within the same straight line with slope = −2.02 and intercept = 5.05 (r^2 = 0.96).

different osm_{out} (0.1 to 1.4 M) and subjected to different tonicity shocks. All the data points fall within the same straight line with a = −2.02 and b = 5.05. Knowing that the relation between V and F is linear, separate calibrations for each stopped-flow trace were done for all cell preparations where epifluorescence microscopy data were available. For other preparations (osm_{out} = 0.2 and 0.4 M) the above values of a and b were used. For any given trace with known tonicity, the initial F corresponding to V/V_o = 1 and final F corresponding to V_∞/V_o taken from the microscopy data (shown in Fig. 1B for osm_{out} = 0.5 and 1.4 M) were used to calculate individual a and b by the relations: $a = (1 - V_\infty/V_o)/(F_o - F_\infty)$ and $b = 1 - aF_o$, increasing in these cases the accuracy of the calibrations.

The evaluation of P_f and L_p followed the approach described in the Materials and methods section. The "*function*" dependence on $1/v$ depicted on Fig. 5 was obtained by plotting Λ vs. $1/v$ taken from

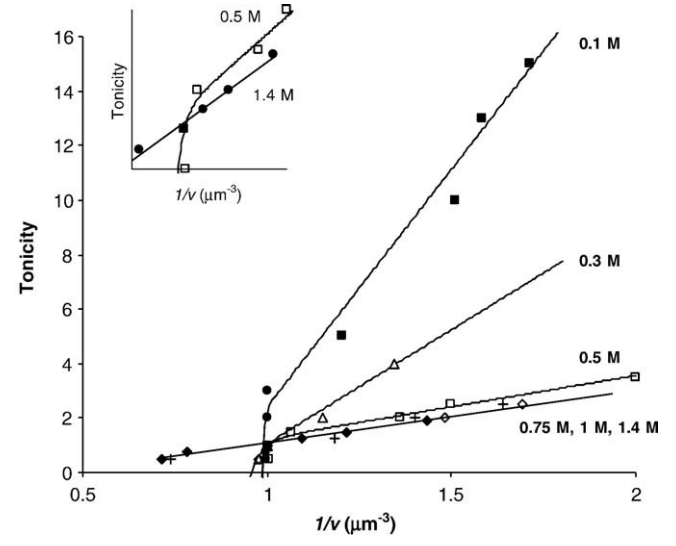

Fig. 5. Tonicity as a function of the reciprocal normalized cell volume $1/v$ (from microscopy volume measurements) for each cell population equilibrated in the different media osmolarities. The obtained "*function*" dependence on $1/v$ (Eq. (5)) accounts for the dissipation of the hydrostatic and osmotic pressures differences during the osmotic equilibration after the onset of the osmotic shock for each cell population. The curves are identified by the osmolarity of the outside medium (osm_{out}). The inset shows a detail of two curves when $1/v$ approaches 1.

microscopy volume measurements for each cell population equilibrated in the different media.

It can be observed that this behaviour is non linear for the cells equilibrated in low osmolarity medium (osm_{out} < 0.75 M) meaning that the pressure terms are not negligible. The values of p_o and β could be estimated for the 1.4 M population by fitting Eq. (4) to the data points where the final pressure after an hyperosmotic shock can be considered to be totally dissipated (p = 0), i.e., the largest hypertonic shocks applied. The value of β = 3.69 µm^3, equivalent to the values obtained for the Boyle–van't Hoff plot for both strains, was obtained together with a very low p_o = 0.1 M.

3.3. Mediated water transport is inhibited by membrane tension

P_f (or L_p) values were calculated for both AQY1 and double mutant *aqy1aqy2* yeast strains. Cell populations were equilibrated in the different external solutions and subjected to hypertonic shocks of different magnitudes that guaranteed the occurrence of measurable volume changes in all cell preparations. The average P_f (or L_p) value for all the osmotic shocks in each cell population was plotted against its preparation buffer osmolarity (osm_{out}). Fig. 6 shows that the calculated P_f (or L_p) values decreased considerably for low external media osmolarity osm_{out} in the AQY1 strain, from $(6.40 \pm 0.33) \times 10^{-4}$ cm s^{-1} ($L_p = (4.68 \pm 0.24) \times 10^{-6}$ cm s^{-1} MPa^{-1}) for osm_{out} 1.4 M (3.40 MPa) to $(2.05 \pm 0.27) \times 10^{-4}$ cm s^{-1} ($L_p = (1.50 \pm 0.19) \times 10^{-6}$ cm s^{-1} MPa^{-1}) for osm_{out} 0.1 M (0.24 MPa). However, no significant change could be observed when the double mutant strain was used in the same experiment, although under the same level of membrane tension. At low osm_{out} the permeability measured for AQY1 strain approaches the double mutant, indicating that the water channels are not functional.

Activation energies (E_a) of osmotic water transport were evaluated. AQY1 and double mutant cells departing from non-tense (equilibrated in 1.4 M) or pre-swollen (equilibrated in 0.5 and 0.3 M) states were subjected to hyperosmotic gradients of different magnitudes. Table 1 shows that for the AQY1 non-tense cells (osm_{out} 1.4 M), the E_a value was low (E_a = 7.2 kcal mol^{-1} (30.1 kJ mol^{-1})), while the double mutant showed a higher value (E_a = 15.1 kcal mol^{-1} (62.8 kJ mol^{-1})) as expected for non-mediated water transport. On the other hand, the E_a value obtained for each population of the AQY1 pre-swollen cells was 10 kcal mol^{-1} (42 kJ mol^{-1}) for the lowest hyperosmotic gradient applied (corresponding to Λ = 1.7 for 0.3 M and Λ = 1.175 for 0.5 M). As the hyperosmotic gradient increased, the E_a decreased approaching the value obtained for

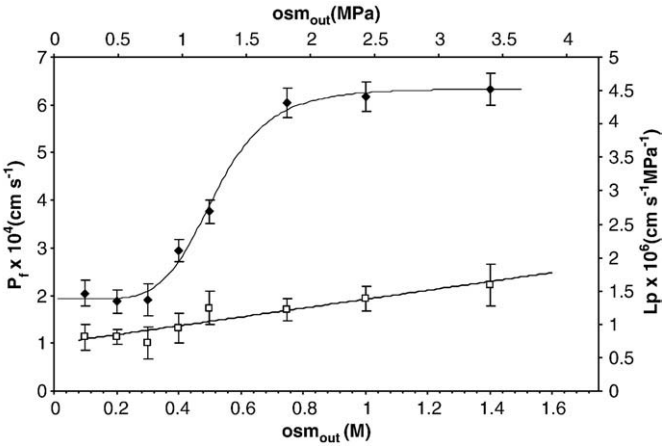

Fig. 6. P_f values (right axis) and L_p (left axis) for *S. cerevisiae* overexpressing *AQY1* (♦) and double mutant *aqy1 aqy2* (□) strains. Both cell strains were equilibrated in the different external solutions (osm_{out} from 0.1 to 1.4 M, bottom axis; 0.24 to 3.4 MPa, top axis) and subjected to hypertonic shocks. Data shown are mean ± SD of triplicates of three independent experiments.

Table 1
Activation energies (E_a) of osmotic water transport for *AQY1* overexpressing and double mutant *aqy1aqy2* strains of *S. cerevisiae* under increasing levels of membrane tension

$(osm_{out})_o$ [M (MPa)]	Tonicity (Λ)	E_a [kcal mol^{-1} (kJ mol^{-1})]	
		Strain AQY1	Strain double mutant
1.4 (3.40)	1.25	7.2 (30.1)	15.1 (63.2)
0.5 (1.21)	4.5	7.2 (30.1)	16.2 (67.8)
	3.5	7.3 (30.5)	
	1.25	8.0 (33.4)	
	1.175	10.0 (41.8)	
0.3 (0.72)	3	7.6 (31.8)	16.2 (67.8)
	1.7	10.2 (42.7)	

cells departing from a non-tense state (for osm_{out} 1.4 M, E_a=7.2 kcal mol^{-1} (30.1 kJ mol^{-1})). Additionally, for these non-tense cells, considering that the double mutant represents only the lipid bilayer contribution for water permeation, the E_a calculated for the channel pathway alone was 4.1 kcal mol^{-1} (17.1 kJ mol^{-1}).

4. Discussion

Under hyperosmotic conditions, mechanisms of osmoregulation comprising the uptake and synthesis of compatible solutes aim to maintain turgor and volume within boundaries acceptable for normal cellular physiology [24]. For hyposmotic stresses, there is evidence for osmoprotectant efflux systems, stretch activated channels, responsible for releasing compatible solutes and restore initial cell volume after the rapid swelling [25]. In intact cells where the cell wall prevents cell bursting, cell swelling is expected under hypotonic conditions up to a maximum volume limited by the cell wall, before the onset of the fast release of compatible solutes. However, for considerable hyposmotic stresses, the regulation process may not fully compensate the large change in cell volume. This condition is evidenced by the initial volume measurements for cells equilibrated in media osmolarities below 0.75 M, where the equilibrium volume remains at its maximum and the cells are thus in a pre-swollen state (Fig. 1A). In these conditions, the hydrostatic pressure is higher within the cell inducing a membrane surface tension. When confronting these cells with a hypotonic shock, as no further increase in volume is possible, the internal hydrostatic pressure increases, further increasing the membrane surface tension. On the other hand, upon a hyperosmotic shock, the initial hydrostatic pressure and the membrane tension start to dissipate. If the magnitude of the shock is sufficient to overcome the hydrostatic pressure difference, the cell shrinks reaching a new equilibrium volume. The larger the tonicity of the osmotic shock, the more efficient it is to dissipate the hydrostatic pressure difference. Figs. 1B and 2 show this behaviour of cell volume change impairment for hypotonic shocks imposed to the pre-swollen cells (equilibrated in 0.5 M) in contrast with the observed volume increase for non-tense cells (equilibrated in 1.4 M). The effect of osm_{out} on the triggering of volume change is emphasized in Fig. 3, where the dependence of the fluorescence signal amplitude on osm_{out} is visualized for different tonicity shocks. This figure points to the fact that the hydrostatic pressure difference increases with the lowering of osm_{out}, resulting in the need of higher tonicity shocks to elicit measurable volume changes upon hyperosmotic challenges. Given a sufficiently large hyperosmotic shock, the final measurable equilibrium volume (where all membrane tension has been dissipated) should be constant for all cell preparations. The V_∞ values in Fig. 1A are in agreement with a cell volume that is still larger than the non-osmotic cell volume calculated (Fig. 1A inset).

Altogether these results point to the existence of a hydrostatic pressure difference between the internal and external media of cells equilibrated in low osmolarity buffers (<0.75 M), keeping the membrane under tension and the cells in a swollen state, being the maximum volume conferred by the cell wall. This hypothesis is supported by previous results with yeast protoplast preparations where a high percentage of cell disruption was observed when 0.8 M sorbitol was used, and stable protoplasts could only be obtained if a concentration of 1.2 M sorbitol was kept throughout the preparation [16].

The linearity between the relative cell volume V/V_o obtained for all the microscopy data and the fluorescence intensity signals from the correspondent stopped-flow experiments (shown in Fig. 4) makes this procedure a tool for calibrating experimental fluorescence stopped-flow data even if microscopy equilibrium volumes are not available.

The P_f evaluation could not be performed using the initial rate constants calculated from single exponential fits to the stopped-flow signals, as frequently applied [26], as the hydrostatic pressure differences have to be taken into account. The method used here includes a "*function*" (Fig. 5) that accounts for the dissipation of the hydrostatic and osmotic pressures differences during the osmotic equilibration after the onset of the osmotic shock, thus enabling accurate calculations of P_f from the calibrated experimental curves. An intuitive explanation for the use of the curves on Fig. 5 to account for the "*function*" behaviour during an osmotic perturbation can be readily understood, considering that the volume changes follow a succession of equilibrium volumes that, at a particular moment during the osmotic perturbation, are in equilibrium with a certain tonicity. For instance, consider that the cells equilibrated in 0.1 M are suddenly exposed to a tonicity shock of Λ=3. The expected volume change of these cells will follow the curve labelled 0.1 M, starting at the point of ($1/v$=1, Λ=1) and ending at the correspondent volume ratio for Λ=3, ($1/v_\infty$, Λ=3). If there were no hydrostatic pressure differences (p_o and p=0) and if the non-osmotic volume was negligible, β=*0*, v_{osm}=v, the "*function*" would reduce to $1/v$, and the curves in Fig. 5 would all reduce to a straight line with a slope of 1 and interception at origin, characteristic of a pure osmometer. As the different curves of Fig. 5 do not fit these conditions, the individual "*function*" terms for each cell population reflect different initial and final pressure values. The value of β obtained both from the Boyle–van't Hoff plot and from the fitting of Eq. (4) to the largest hypertonic shocks of 1.4 M population (Fig. 5), gave identical estimates for the non-osmotic volume.

The increase in P_f values with osm_{out} (Fig. 6) suggests that cells overexpressing *AQY1* that depart from a pre-swollen state and thus bare an initial membrane surface tension have lower water permeabilities. When the external osmolarity is as low as 0.3 M, the P_f measured for these cells approaches the one obtained for the double mutant. A similar phenomenon has been previously reported for vesicles derived from kidney brush border vesicles, where the increase in membrane surface tension decreased water flow through water channels [20,21].

Further evidence for the effects of membrane tension on water channel activity is seen when activation energies from cells equilibrated in different osm_{out} are compared. This pattern is demonstrated in Table 1 where water channels show different levels of inhibition (higher E_a values) depending on the efficiency of hydrostatic pressure dissipation. Moreover, the E_a calculated for the channel pathway was similar to the reported for the activation energy of water transport through water channels [4].

Aquaporins are ubiquitous and their role as water channels has been recognized in nature. In 2004 Hill et al. suggested that aquaporins could also function as osmotic and turgor sensors [19]. The results presented in this paper offer evidence that yeast aquaporins are sensitive to membrane tension and this could be a mechanism that, in cooperation with other osmosensitive solute transporters, aim to preserve cell volume. In fact, both the water channel and solute pumping mechanisms require time for water equilibration, but in addition the pumping mechanisms also require time to pump solutes, which is generally much slower than water equilibration. Thus we can expect the water channel mechanism to

provide a more rapid response. Under hyposmotic conditions, the rapid increase in cell volume and consequent development of membrane tension would inhibit membrane water permeability, slowing water fluxes, in order to maintain a suitable cell volume while solute pumping is being triggered. The impairment of water transport by membrane tension would be the first available volume regulatory tool to avoid drastic cell swelling.

Acknowledgements

This work was supported by Fundação para a Ciência e Tecnologia, POCTI/AGR/57403/2004. We thank Doctor Paulo Costa Lemos, REQUIMTE, Portugal, for the supervision on the epifluorescence experiments.

References

[1] C.V. Paganelli, A.K. Solomon, The rate of exchange of tritiated water across the human red cell membrane, J. Gen. Physiol. 41 (1957) 259–277.
[2] F.L. Vieira, R.I. Sha'afi, A.K. Solomon, The state of water in human and dog red cell membranes, J. Gen. Physiol. 55 (1970) 451–466.
[3] R.E. Farmer, R.I. Macey, Perturbation of red cell volume: rectification of osmotic flow, Biochim. Biophys. Acta 196 (1970) 53–65.
[4] R.I. Macey, D.M. Karan, R.E. Farmer, Properties of water channels in human red cells, Biomembranes 3 (1972).
[5] A.S. Verkman, Water channels in cell membranes, Annu. Rev. Physiol. 54 (1992) 97–108.
[6] G.M. Preston, T.P. Carroll, W.B. Guggino, P. Agre, Appearance of water channels in *Xenopus* oocytes expressing red cell CHIP28 protein, Science 256 (1992) 385–387.
[7] Q. Ye, B. Wiera, E. Steudle, A cohesion/tension mechanism explains the gating of water channels (aquaporins) in Chara internodes by high concentration, J. Exp. Bot. 55 (2004) 449–461.
[8] X. Wan, E. Steudle, W. Hartung, Gating of water channels (aquaporins) in cortical cells of young corn roots by mechanical stimuli (pressure pulses): effects of ABA and of HgCl2, J. Exp. Bot. 55 (2004) 411–422.
[9] F. Chaumont, M. Moshelion, M.J. Daniels, Regulation of plant aquaporin activity, Biol. Cell. 97 (2005) 749–764.
[10] A. Tanghe, P. Van Dijck, J.M. Thevelein, Why do microorganisms have aquaporins? Trends. Microbiol. 14 (2006) 78–85.
[11] M. Bonhivers, J.M. Carbrey, S.J. Gould, P. Agre, Aquaporins in *Saccharomyces*. Genetic and functional distinctions between laboratory and wild-type strains, J. Biol. Chem. 273 (1998) 27565–27572.
[12] J.M. Carbrey, M. Bonhivers, J.D. Boeke, P. Agre, Aquaporins in *Saccharomyces*: characterization of a second functional water channel protein, Proc. Natl. Acad. Sci. U. S. A. 98 (2001) 1000–1005.
[13] V. Laizé, F. Tacnet, P. Ripoche, S. Hohmann, Polymorphism of *Saccharomyces cerevisiae* aquaporins, Yeast 16 (2000) 897–903.
[14] F. Sidoux-Walter, N. Pettersson, S. Hohmann, The *Saccharomyces cerevisiae* aquaporin Aqy1 is involved in sporulation, Proc. Natl. Acad. Sci. U. S. A. 101 (2004) 17422–17427.
[15] A. Tanghe, P. Van Dijck, D. Colavizza, J.M. Thevelein, Aquaporin-mediated improvement of freeze tolerance of *Saccharomyces cerevisiae* is restricted to rapid freezing conditions, Appl. Environ. Microbiol. 70 (2004) 3377–3382.
[16] G. Soveral, A. Veiga, M.C. Loureiro-Dias, A. Tanghe, P. Van Dijck, T.F. Moura, Water channels are important for osmotic adjustments of yeast cells at low temperature, Microbiology 152 (2006) 1515–1521.
[17] E.K. Hoffmann, Intracellular signalling involved in volume regulatory decrease, Cell. Physiol. Biochem. 10 (2000) 273–288.
[18] S. Hohmann, M. Krantz, B. Nordlander, Yeast osmoregulation, Methods Enzymol. 428 (2007) 29–45.
[19] A.E. Hill, B. Shachar-Hill, Y. Shachar-Hill, What are aquaporins for? J. Membr. Biol. 197 (2004) 1–32.
[20] G. Soveral, R.I. Macey, T.F. Moura, Water permeability of brush border membrane vesicles from kidney proximal tubule, J. Membr. Biol. 158 (1997) 219–228.
[21] G. Soveral, R.I. Macey, T.F. Moura, Membrane stress causes inhibition of water channels in brush border membrane vesicles from kidney proximal tubule, Biol. Cell 89 (1997) 275–282.
[22] G. Soveral, A. Madeira, M.C. Loureiro-Dias, T.F. Moura, Water transport in intact yeast cells as assessed by fluorescence self-quenching, Appl. Environ. Microbiol. 73 (2007) 2341–2343.
[23] A. Tanghe, P. Van Dijck, F. Dumortier, A. Teunissen, S. Hohmann, J.M. Thevelein, Aquaporin expression correlates with freeze tolerance in baker's yeast, and overexpression improves freeze tolerance in industrial strains, Appl. Environ. Microbiol. 68 (2002) 5981–5989.
[24] B. Kempf, E. Bremer, Uptake and synthesis of compatible solutes as microbial stress responses to high-osmolality environments, Arch. Microbiol. 170 (1998) 319–330.
[25] E. Glaasker, W.N. Konings, B. Poolman, Glycine betaine fluxes in *Lactobacillus plantarum* during osmostasis and hyper- and hypo-osmotic shock, J. Biol. Chem. 271 (1996) 10060–10065.
[26] V. Laizé, R. Gobin, G. Rousselet, C. Badier, S. Hohmann, P. Ripoche, F. Tacnet, Molecular and functional study of AQY1 from *Saccharomyces cerevisiae*: role of the C-terminal domain, Biochem. Biophys. Res. Commun. 257 (1999) 139–144.